LAWRENCE
LIVERMORE
NATIONAL
LABORATORY

LLNL-JRNL-646555

Symmetry Control of Imploding Capsules at the National Ignition Facility using 2D X-ray Radiography

J. R. Rygg, O. S. Jones, J. E. Field, M. A. Barrios, L. R. Benedetti, G. W. Collins, D. C. Eder, M. J. Edwards, J. L. Kline, J. J. Kroll, O. L. Landen, T. Ma, A. E. Pak, L. Peterson, K. Raman, R. P. J. Town, D. K. Bradley

November 19, 2013

Physical Review Letters

Disclaimer

Symmetry control of imploding capsules at the National Ignition Facility using 2D x-ray radiography

J. R. Rygg,[1] O. S. Jones,[1] J. E. Field,[1] M. A. Barrios,[1] L. R. Benedetti,[1] G. W. Collins,[1] D. C. Eder,[1] M. J. Edwards,[1] J. L. Kline,[2] J. J. Kroll,[1] O. L. Landen,[1] T. Ma,1 A. Pak,[1] L. Peterson,[1] K. Raman,[1] R. P. J. Town,[1] and D. K. Bradley[1]
[1]*Lawrence Livermore National Laboratory, Livermore, CA 94551, USA*
[2]*Los Alamos National Laboratory, Los Alamos, NM* 87545, USA
(Submitted to Phys. Rev. Lett. on 25 Nov 2013)

First measurements of the in-flight shape of imploding inertial confinement fusion (ICF) capsules at the National Ignition Facility (NIF) were obtained using 2-dimensional x-ray radiography. The sequence of area-backlit, time-gated pinhole images is analyzed for implosion velocity, low-mode shape and density asymmetries, and the absolute offset and drift velocity of the capsule shell. The in-flight shell is often observed to be asymmetric even when the concomitant core self-emission is round. A ~15 μm shell asymmetry amplitude of the Y_{40} spherical harmonic mode was observed for standard NIF ICF hohlraums at a shell radius of ~200 μm. This asymmetry was mitigated by a ~10% increase in the hohlraum length.

In pursuit of inertial confinement fusion (ICF) [1,2] ignition at the National Ignition Facility (NIF) [3], spherical capsules are filled with deuterium-tritium (DT) fuel and imploded using the x-ray radiation drive produced inside laser-heated cylindrical hohlraums. Successful ignition requires a high degree of spherical symmetry to maximally compress the DT fuel within the capsule. Low-mode shape distortions as the capsule implodes will diminish the conversion efficiency of the imploding fuel kinetic energy; some energy that would convert into internal energy of the core hot-spot will instead result in transverse motion of the capsule shell [1,2] These shape distortions will further degrade fusion yield performance by reducing the confinement time of the compressed fuel [1,2].

Earlier efforts at the NIF were able to tune out the observed low-mode asymmetry of x-ray self-emission from the core at stagnation [4]. However, the continued presence of residual low-mode asymmetry in the imploded shell has been conjectured as a contributor to the degraded fusion yield observed in NIF implosions compared to simulations [5]. In this Letter, we present the first 2D radiography experiments of imploding ignition-scale capsules at peak velocity at the NIF, and report the measurement and mitigation of previously undetected low-mode asymmetry in the in-flight capsule shell. Through characterization of low-mode in-flight shape of the capsule shell, this 2D radiography platform enables control of low-mode shell asymmetry in ICF capsules that is critical to achieve fusion ignition.

The shape of imploding ICF capsules is often decomposed into spherical harmonics $Y_{\ell m}$, the azimuthally-symmetric of which ($Y_{\ell 0}$) are represented by the Legendre polynomials P_ℓ. If the capsule is initially very symmetric, low-mode distortions of the shape are caused by non-uniformity of the x-ray drive, which is a function of the intensity and geometry of the laser spots on the hohlraum wall. Previous experiments on the Nova laser [6] demonstrated control of capsule P_2 in a hohlraum heated by two rings (or cones) of beams [7], as diagnosed by x-ray self-emission of the stagnated capsule. The NIF heats the hohlraum with 4 rings rather than 2, which can in principle control both P_2 and P_4 by properly choosing the locations of the rings and varying the power between cones.

Time-dependent drive symmetry has previously been measured using backlit imaging of a low-density foam ball [8,9,10] and thin-shell [11,12,13] surrogate targets, including demonstration of P_2 control in multi-cone experiments. More recently at the NIF a technique was developed [14,15] to measure the time-dependent trajectory and velocity of an imploding ignition-scale ICF capsule using 1-dimensional x-ray radiography [14,15].

The experimental setup reported herein has much in common with that described in references [14] and [15], with a NIF ignition-scale target [1] modified for backlit imaging (Fig. 1). In this case, the target consists of a cylindrical gold hohlraum with 5.75 mm inner diameter and inner length between 9.13 and 10.43 mm. A 1.15 mm outer radius, 0.21 mm thick plastic spherical shell is held at the center of the hohlraum by two thin (~45 nm) plastic membranes. The capsule shell is filled with 6.7 mg/cm^3 of 30%at D_2 and 70%at ^{3}He gas when cooled to 24 K. The hohlraum is driven with a 1.3 MJ, 21 ns long, shaped ignition pulse (Fig. 1) [1].

Eight of NIF's 192 beams are redirected from the hohlraum to a germanium foil 12 mm from the capsule center in the equatorial plane. To partially compensate for the 8 missing beams, power is increased by an average of 12.5% on 64 of the nearby beams. The pulse shape of the 8 backlighter (BL) beams incident on the Ge foil is tuned to produce maximum brightness in the 10.25 keV Ge He-α line, as discussed in Ref [16] and adapted for NIF as described in Ref [17]. The backlighter x-ray line energy is chosen to match the expected capsule opacity, giving about 1 optical depth of absorption through the capsule limb. The backlighter's 52 kJ laser energy is converted with about 1% efficiency into the Ge He-α line, creating an x-ray emission area approximately 1 mm in diameter and 2 ns in duration.

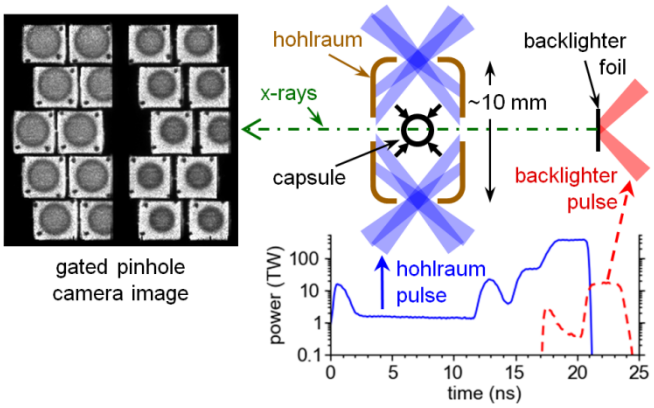

Fig. 1. A ~10 mm long cylindrical hohlraum converts 1.3 MJ of laser energy into a ~300 eV radiation drive and implodes a 2.3 mm diameter spherical capsule. A backlighter foil 12 mm away in the equatorial plane is illuminated with additional laser beams as the capsule implodes, generating backlit images of the in-flight capsule on a time-gated pinhole camera. Capsule transmission is deduced after compensating for backlighter non-uniformities (see text).

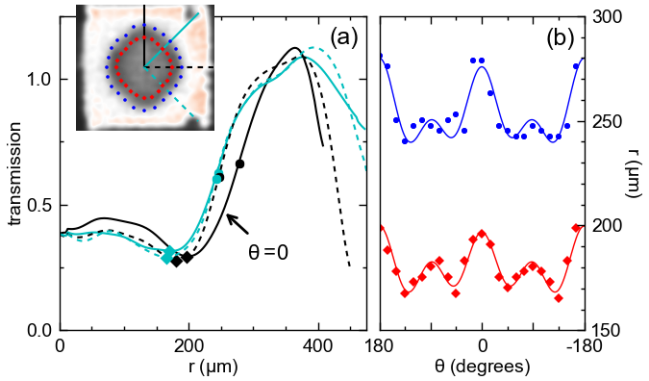

Fig. 2. (a) Four radial lineouts of frame (inset) sectors are analyzed for the radii corresponding to the limb minimum (diamonds) and max slope (circles). (b) The limb minimum (red) and maximum slope (blue) contours are fit with Legendre polynomial to characterize the low-mode shape of the inflight capsule shell.

To provide a line-of-sight from the Ge BL foil through the capsule to the detector, two 0.9×0.83 mm viewing holes are cut out of opposite sides of the hohlraum wall. Two 0.8 mm square high-density carbon (HDC) windows are inserted into the cutouts to prevent premature closure of the viewing holes. Low-transmission, 0.1 mm diameter fiducial dots are placed in the corners of the HDC squares to relate the absolute and initial positions of the imploding capsule.

Area-backlit images of the imploding capsule (Fig. 1) are created by pinhole projection onto a gated x-ray detector [18] at 8x magnification. The detector has two microchannel plate (MCP) striplines with a temporal integration time of approximately 90 ps. The two MCP strips as well as the BL pulse are timed to coincide with capsule in-flight shell radii between 300 and 150 μm. Discrete image frames are generated through the individual, 20-25 μm diameter pinholes in a pinhole array. Often visible is a pair of horizontal bands at approximately half the capsule radius that are seeded by the plastic membranes that initially hold the capsule at the center of the hohlraum [19].

Data images consist of multiple time-gated image frames generated by these individual pinholes. The image frame intensities are converted to capsule transmission using pinhole tomography. The tomographic method takes advantage of the slight parallax difference between the backlighter and capsule object planes for each pinhole in the pinhole array to distinguish features originating in the respective planes.

To evaluate the shape of the in-flight shell, each frame is divided into angular sectors, and the radial lineout for each sector is analyzed for the limb minimum and maximum slope radii (Fig. 2a). These radii correspond approximately to the inner and outer boundaries of the shell, respectively. The limb-minimum and maximum-slope contours constructed from these radii of all angular sectors are each fit with a Legendre polynomial series (Fig. 2b) [20]:

$$r(\theta) = \sum_\ell A_\ell P_\ell(\cos\theta). \qquad (1)$$

The fit averages over any left-right asymmetry, which is typically smaller than the fit uncertainty. Evolution of the low-mode capsule shape as it implodes, including the dA_0/dt "implosion velocity," is obtained by sequential analysis of the image frames. Areal density can be inferred from the capsule transmission with a suitable assumption of the shell opacity [14,15], giving a typical shell-averaged areal density of ~0.1 g/cm^2 for these capsules at the time of the radiograph. Detailed results of the areal density symmetry analysis for the 2D radiographs will be reported elsewhere.

Additionally, the spatially and temporally resolved radiograph is used to measure a bulk capsule velocity. Such velocity can be imparted by large asymmetries in the radiation flux and is expected to reduce the compression and yield of implosions. The absolute position and drift velocity of the capsule limb are measured in reference to the fiducial dots placed on the HDC windows [21], whose shadow positions can be determined to ±10 μm. Comparison of the absolute position of the capsule at the beginning and end of the ~0.4 ns frame sequence allows us to constrain the drift velocity of the capsule to ~10 km/s. Typically, the center of the imploded capsule is within 15 μm of the initial capsule center, and is moving with a speed less than 20 km/s within the plane transverse to the line of sight. The associated center-of-mass kinetic energy represents less than 1% of the kinetic energy of the imploding shell.

As a first demonstration of this NIF 2D radiography platform, a campaign was undertaken which confirmed the conjectured presence of an in-flight P4 distortion of the shell [5]. In this conjectured scenario, the observed hot-spot self-emission symmetry could still appear round due to a mixture of various low-mode components in the shell. Previous experiments had tuned out low-mode shape perturbations based on the hot-spot self-emission measurements, and selected a hohlraum length of 9.43 mm to produce optimal control of P_2 asymmetry for a hohlraum inner diameter of 5.75 mm [22]. However, the symmetry of the assembled cold fuel could not be conclusively demonstrated without a direct measurement of the shell; this 2D radiography platform was used to make such a measurement at the NIF.

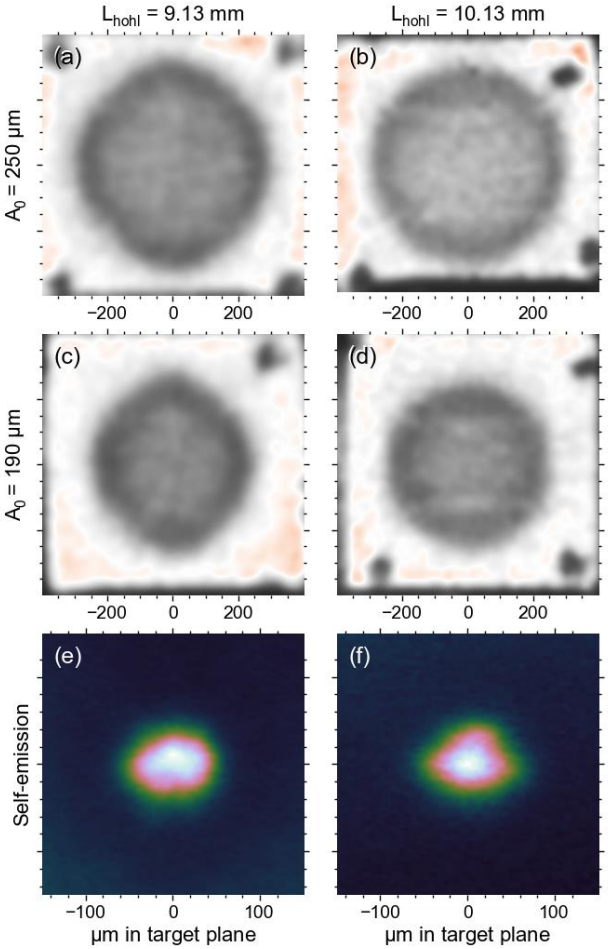

Fig. 3. (a-d) Backlit radiographs of the capsule in-flight when the first Legendre mode amplitude $A_{0,limbmin}$ = 250 and 190 μm. Two hohlraum lengths are shown that differ by 1 mm (~10%). A ~17 μm A_4 component is reduced below 5 μm with the longer hohlraum. (e,f) Concomitant time-integrated self-emission images often exhibit different low-mode shape than the in-flight shell radiographs. Note change in spatial scale for (e,f).

To evaluate the shell symmetry, a sequence of otherwise-identical shots was performed in which the hohlraum length L varied from 9.13 to 10.43 mm. The outer cone beams were kept at the same position with respect to the laser entrance holes (LEH) by repointing them by half the difference in L. The 64 inner cone beams kept the same pointing near the hohlraum mid-plane, independent of hohlraum length. The shell implosion velocity is the same for all experiments in this campaign at 285 ± 12 km/s, and is constant for the ~0.4 ns duration of the radiographic window. In addition to the in-flight 2D radiography measurement, time-integrated self-emission [23] images were measured concomitantly from the same line of sight.

As seen in Fig. 3, the shape of the capsule shell often differs dramatically from the shape of the x-ray emission from the hot core. In particular, the short (9.13 mm long) hohlraum experiment results in an imploding shell that primarily exhibits a positive P_4 (a,c), whereas the resultant self-emission is dominated by a negative P_2 (e). This result suggests that contours of the self-emission are not reflective of the shape of the stagnated ablator shell.

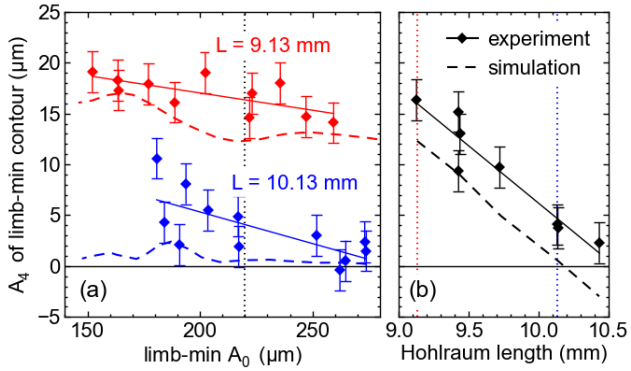

Fig. 4. (a) Evolution of capsule shape as it implodes over ~0.4 ns for two different hohlraum lengths L. (b) In-flight capsule A_4 at A_0 = 220 μm is reduced to within 5 μm of "round" for L ~1 mm longer than the previous standard. Solid lines are linear fits to the data. Hydro simulations (dashed lines) get the correct scaling of A_4 with L, but with an offset in the absolute A_4 amplitude.

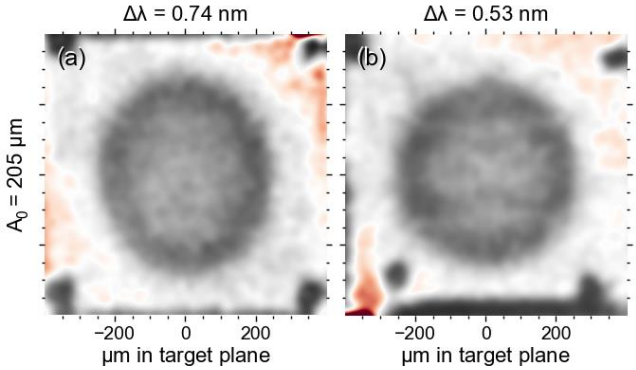

Fig. 5. Backlit radiographs of capsule in-flight when $A_{0,limbmin}$ = 205 μm. Both experiments used 10.13 mm long hohlraums. The difference in laser wavelength between inner and outer cones (Δλ) affects the transfer of energy between cones. This mechanism is used to control Legendre mode P_2, here reducing the A_2 component from 25 to 1 μm.

Fig. 4 shows the radial evolution of the A_4 fit to the limb-minimum contour as the capsule implodes. Also shown is the dependence of A_4 on hohlraum length. A shell A_4 of 13 μm is observed for the 9.43 mm length hohlraum experiment when the capsule radius is at 220 μm (~0.6 ns before shell stagnation). The residual P_4 asymmetry is mitigated by a ~1 mm increase in hohlraum length.

The scaling of the in-flight P_4 with hohlraum length can be understood qualitatively using a simplified spherical model of the hohlraum [1]. In this model, the P_4 component of the radiation flux seen by the capsule is a balance of contributions from the laser-heated emission ring near the hohlraum equatorial plane, the two emission rings from the outer cone beams on each side, and the re-radiation from the hohlraum wall. As the hohlraum is lengthened and the outer rings move outwards, the simple geometric model shows that both the outer rings and the wall re-radiation terms contribute additional positive P_4 to the capsule radiation flux. The capsule in-flight shape responds to low-mode flux asymmetries with opposite sign, as the higher flux regions are driven to smaller radius. In this case, the larger P_4 flux from the longer hohlraum reduces the in-flight capsule P_4.

This model also anticipates a negative P_2 contribution as hohlraum length increases. However, as previously reported for self-emission measurements [4], P_2 can be independently controlled by means of laser wavelength adjustments. Energy is transferred between inner and outer laser beams by a plasma wave self-generated where the beams cross near the LEHs [26]. This cross-beam energy transfer (CBET) depends in part on the difference in laser wavelength between inner and outer beams $\Delta\lambda$. As seen in Fig. 5, a reduction of the measured shell A_2 from 25 to 1 μm can be achieved with an adjustment of 0.21 nm in $\Delta\lambda$.

An additional observation is the ~6 μm increase in A_4 as the capsule implodes over the ~0.4 ns time window of the measurement, indicating a P_4 swing of ~15 μm/ns. This observed P_4 swing rate is not strongly correlated with hohlraum length. Our simple model is time-independent, so cannot explain this P_4 swing.

To understand the cause of this P_4 swing as well as the observed change due to hohlraum length, simulations were done using the radiation hydrodynamics code Hydra [25]. The hohlraum and capsule are calculated together in a single self-consistent calculation – that is, the laser refraction, absorption and subsequent conversion to x-rays near the high-Z hohlraum wall are calculated directly, and those x-rays then are transported to the capsule ablation surface and drive the capsule inwards.

The cross-beam energy transfer (CBET) is modeled in a separate calculation [26] using plasma parameters extracted from a Hydra simulation with no laser backscatter removed. The calculated CBET at high power during the peak of the laser pulse is generally larger than inferred from experiment and so is moderated by setting a threshold density perturbation value (dn/n) for the CBET [26]. When the resonant process that drives CBET causes the local dn/n to exceed that threshold, no further transfer is allowed in that portion of the laser beam crossing volume.

A second Hydra calculation is then done with the measured input laser power modified by the measured laser backscatter and calculated crossbeam energy transfer. The input drive is further modified in order to match shock timing, trajectory, and neutron bang time data from other experiments [27]. We set the peak power dn/n to 4.0e-4 for these calculations in order to match the P2 moment of the measured inflight shape.

Hydra simulations with the CBET model reproduce the observed scaling of the in-flight capsule P4 with hohlraum length, but have an offset as to the absolute magnitude (Fig. 4b). Simulations anticipate that the P4 time-dependent swing is reduced for longer hohlraums, in contrast to the measurements which demonstrate no such reduction. The reason for the difference between the in-flight and self-emission shape is an area of active investigation, but may originate in a time-dependent transfer of energy between the inner and outer cones. Improvement to Hydra and the CBET model is ongoing, with in-flight 2D radiography playing a key role to constrain the power-dependent saturation.

In summary, a new experimental platform was developed at the NIF for 2D radiography of imploding capsules in-flight. It was demonstrated that the shape of the hot-spot self-emission can be misleading as to the symmetry of the surrounding cold shell. The dependence of the in-flight shell shape on hohlraum length was measured, and the optimum length to minimize the spherical harmonic mode Y_{40} was determined to be ~10% longer than the previous optimum determined solely through self-emission shape measurements. Residual temporal swings in the low modes remain, which may be due in part to time-dependence of cross-beam energy transfer between inner and outer drive beams. Results from this platform are being used in an ongoing manner to improve several models used in ICF simulation and design codes, and to determine the implosion velocity, drift velocity, areal density, and low-mode shape of the imploding capsule shell for new ICF configurations at the NIF.

The authors would like to thank the engineering, target fabrication, and operations teams at the National Ignition Facility who made these experiments possible. This work was performed under the auspices of the U.S. Department of Energy by Lawrence Livermore National Laboratory under Contract DE-AC52-07NA27344.

---

[1] J. Lindl, Phys. Plasmas 2, 3933 (1995); ibid 11, 339 (2004).
[2] S. Atzeni and J. Meyer-ter-Vehn, *The Physics of Inertial Fusion* (Oxford University Press, Oxford, UK, 2007).
[3] G. H. Miller, E. I. Moses, and C. R. Wuest, Nucl. Fusion 44, S228 (2004).
[4] S. H. Glenzer et al., Science 327, 1228 (2010).
[5] R. H. H. Scott et al, Phys. Rev. Lett. 110, 075001 (2013).
[6] E. M. Campbell, et al., Rev Sci Instr 57, 2101 (1986).
[7] P. Amendt, T. J. Murphy, and S. P. Hatchett, Phys Plasmas 3 (11), 4166 (1996).
[8] P. A. Amendt, et al., PRL 77 (18) 3815 (1996).
[9] S. G. Glendinning et al, Rev. Sci. Instrum. 70, 536 (1999).
[10] R. E. Turner, et al., Phys Plasmas 10, 2429 (2003)
[11] D. H. Kalantar et al, Rev. Sci. Instrum. 68, 814 (1997).
[12] S Pollaine et al, Phys Plasmas 8, 2357 (2001).
[13] R. Kirkwood et al, Phys Plasmas 16, 012072 (2009).
[14] D. G. Hicks et al, Phys. Plasmas 17, 102703 (2010).
[15] D. G. Hicks et al, Phys. Plasmas 19, 122702 (2012).
[16] D. Babonneau et al, Phys. Plasmas 15, 092702 (2008).
[17] M. A. Barrios et al, High Energy Density Phys. 9, 626 (2013).
[18] J. A. Oertel et al, Rev. Sci. Instrum 77, 10E308 (2006).
[19] The membrane was conclusively identified as the origin of these bands by two independent sets of experiments, to be published elsewhere. In most cases, this feature has only a small effect on the inferred in-flight shape.
[20] The Legendre-mode shape breakdown is insensitive to the application of the tomographic step.
[21] Only the components of position and velocity transverse to the line of sight are directly observed.
[22] D. A. Callahan et al., Phys. Plasmas 19, 056305 (2012).
[23] T. Ma et al, Rev. Sci. Instrum. 83 10E115 (2012).
[24] G. Kyrala et al, Phys. Plasmas 18, 072703 (2011).
[25] M. M. Marinak, G. D. Kerbel, N. A. Gentile, et al., Phys. Plasmas 8, 2275 (2001).
[26] P. Michel, S. H. Glenzer, L. Divol, et al., Phys. Plasmas 17, 056305 (2010).
[27] O. S. Jones et al., Phys. Plasmas 19, 056315 (2012).